ISSN 1027-5495. Functional Materials, 28, No.1 (2021), p. 187-195.
doi:https://doi.org/10.15407/fm28.01.187

The effect of UV and glow-discharge hydrogen plasma irradiation on the crystalline structure and efficiency of CdTe/CdS thin film solar cells prepared by the quasi-closed volume method

***M.M.Harchenko*[1], *A.V.Meriuts*[1], *A.V.Nikitin*[2], *S.V.Surovitskiy*[1], *A.I.Dobrozhan*[1], *Y.V.Buts*[3]**

[1]National Technical University "Kharkiv Polytechnic of Institute", 2 Kyrpychova Str., 61002 Kharkiv, Ukraine
[2]National Science Center "Kharkiv Institute of Physics & Technology", 1 Academicheskaya Str., 61108 Kharkiv, Ukraine
[3]S. Kuznets Kharkiv National University of Economics, 9-A Nauka Ave., 61166 Kharkiv, Ukraine

Received June 14, 2020

It is shown that the crystal structure and photoelectric properties of CdS/CdTe-based solar cells (SCs), fabricated by condensation in a quasi-closed volume, change their characteristics the action of irradiation with a high-dose hydrogen plasma flux. At the same time, the characteristics of these SCs turn out to be insensitive to UV radiation. The change in the structural characteristics under the action of hydrogen plasma is due to the heating factor at a high flux density of ~ $8{\cdot}10^{18}$ $cm^{-2}c^{-1}$ and hydrogen diffusion to the CdS/CdTe interface, while the degradation of the photoelectric characteristics is mainly associated with physical destruction of the back contact due to its plasma etching.
Keywords: solar cells, irradiation, crystal structure, photoelectric characteristics.

Вплив опромінення ультрафіолетом і низько енергетичною водневою плазмою на кристалічну структуру базового шару і ефективність плівкових сонячних елементів на основі телуриду і сульфіду кадмію, виготовлених методом конденсації у квазізамкнутому об'ємі, *М.М.Харченко, А.В.Меріуц, А.В.Нікітін, С.В.Суровицький, А.І.Доброжан, Ю.В.Буц*

Показано, що кристалічна структура і фотоелектричні властивості сонячних елементів на основі CdS/CdTe, виготовлених методом конденсації у квазізамкнутом об'ємі, змінюють свої характеристики під дією опромінення потоком водневої плазми з великими дозами. В той же час, характеристики цих сонячних елементів виявилися мало чутливими до ультрафіолетового опромінення. Зміна структурних характеристик під дією водневої плазми обумовлена фактором розігріву при високій густині потоку ~ $8{\cdot}10^{18}$ $cm^{-2}c^{-1}$ і дифузією водню до границі розділу CdS/CdTe, в той час як деградація фотоелектричних характеристик в основному пов'язана з фізичним руйнуванням тильного контакту за рахунок його травлення плазмою.

Показано, что кристаллическая структура и фотоэлектрические свойства солнечных элементов на основе CdS/CdTe, изготовленных методом конденсации в квазизамкнутом объеме, изменяют свои характеристики под действием облучения потоком водородной плазмы с большими дозами. В то же время, характеристики этих солнечных элементов оказываются малочувствительными к ультрафиолетовому излучению. Изменение струк-

турных характеристик под действием водородной плазмы обусловлено фактором разогрева при высокой плотности потока ~ $8 \cdot 10^{18}$ $cm^{-2}c^{-1}$ и диффузией водорода к границе раздела CdS/CdTe, в то время как деградация фотоэлектрических характеристик в основном связана с физическим разрушением тыльного контакта за счет его травления плазмой.

1. Introduction

Due to the low consumption of materials and energy, thin-film [1–3] and nanostructured solar cells (SCs) [4] currently successfully compete with instrument structures based on crystalline silicon under terrestrial conditions. One of the problems that must be solved for the space application of any types of solar cells or when using them under conditions of increased radiation is the development of constructional and technological solutions aimed at minimizing the degradation processes of the output parameters of the instrument structures. For example, in order to improve degradation resistance of silicon based solar cells, diamond-like carbon films may be applied [5–7]. The films improve not only the SC efficiency owing to decreasing reflection losses and the SC surface passivation [5], but their radiation resistance against gamma and ultraviolet (UV) irradiations as well [6, 7]. Among thin-film solar cells, the instrumental structures based on cadmium telluride are most promising for use under conditions of increased radiation. They exhibit the highest degradation resistance under the action of protons and electrons in comparison with crystalline SCs based on silicon and film SCs based on other semiconductor base layers, as was experimentally established in [8]. In this work, it was shown that a change in the parameters of solar cells quantitatively correlates with the number of recombination centers. In the case of proton irradiation, passivation of recombination centers at low and medium proton fluxes was established, and the exponential dependence of the recovery of the output parameters of damaged spacecraft on time was shown. It was shown in [9] that a decrease in the short circuit current of cadmium telluride film solar cells is the main factor in reducing their efficiency when irradiated with high-energy protons.

The prospect of the space application of film SCs based on cadmium telluride is also due to the technologies currently being developed to create such instrument structures on flexible substrates; this allows you to achieve record values of electric power per unit weight. Reducing the weight of solar cells can reduce the cost of putting the solar battery into orbit.

The aim of this work is to study the effects of irradiation with UV large doses and low-energy hydrogen plasma on the crystal structure of the base layer and the output parameters of cadmium telluride based SCs.

2. Experimental

Cadmium telluride film solar cells were formed on a glass substrate with a previously applied transparent and conductive FTO layer, which performs the functions of a front electrode in the instrument structure. The surface resistance of the FTO layer was 10–12 Ω/□, and the average transmission coefficient in the visible part of the spectrum was 80–85 %. The sequence of operations in the manufacture of the solar cells is as follows: deposition of CdS and CdTe layers; "chloride" treatment; creating a back contact.

The cadmium sulfide and cadmium telluride layers were deposited by condensation in a quasi-closed volume (QCV), which allows deposition under conditions close to thermodynamically equilibrium. The layers were deposited sequentially without depressurization of the working volume at a residual gas pressure of no higher than 10^{-5} mm Hg. Two separate graphite chambers located in the working volume of an industrial vacuum installation were used. The methodology for applying the layers is described in detail in [10].

When the CdS layers were deposited, the temperature of the zone of the evaporator was 590°C, and the temperature of the substrate was 395°C, which corresponds to quasi-equilibrium condensation conditions. With a condensation process duration of 15 min, CdS films 0.3–0.32 μm thick were obtained. In [11], it was shown that CdS layers deposited in this mode are free from metastable cubic modification and contain only the hexagonal CdS modification; the average grain size is 400–500 nm. The predominant grain orientation with the *c* axis close to the normal to the surface of the substrate is observed in the layers. In the spectral range of wavelengths of 550–1100 nm, the average transmittance of the films is 70 %, which ensures the arrival of

a high photon flux density in the spectral range of the photosensitivity of the cadmium telluride base layer. The band gap determined from the position of the edge of the absorption band, is 2.41–2.43 eV.

The CdTe layers were deposited at a temperature of the evaporation zone of 520°C and a substrate temperature of 497°C. In this temperature regime, with a duration of the condensation process of 7 min, CdTe films with a thickness of 3.8–4 μm and grain sizes of 3–5 μm at the surface were obtained. It was shown in [10] that CdTe films obtained by condensation in QCV do not contain a hexagonal modification. Therefore, the analysis of the diffraction patterns of the samples below was performed for the cubic phase of CdTe.

The "chloride" treatment consisted in the deposition of a $CdCl_2$ film on the surface of a CdTe film by thermal vacuum evaporation without heating the substrate and annealing the entire structure in air at a temperature of 410–415°C and a duration of 20 min. After annealing, the surface was etched in a solution of bromine in methanol to remove the products of a chemical reaction.

The back contact was formed by depositing copper and gold films with a thickness of 11 nm and 50 nm, respectively, followed by annealing of the structure in air at a temperature of 230°C for 20 min. The copper and gold films were deposited by vacuum thermal evaporation in a single cycle at a pressure of no higher than 10^{-5} mm Hg without heating the substrate. The thickness of the layers was monitored by a quartz thickness gauge.

After this, some of the samples were subjected to UV irradiation with a quantum energy of 10 eV, a flux density of 10^{20}–10^{21} quanta·m^{-2}s^{-1} for 12 hours, which corresponds to an irradiation dose of $5 \cdot 10^6$ Gray. The irradiation was carried out in air from the contact side, since the glass substrate blocks UV radiation; while the gold contact with a thickness 0.1 μm, which is less than the wavelength of the incident radiation, could partially transmit radiation. For control, a section of the structure without a back contact was also exposed to radiation.

For the hydrogen plasma treatment of the solar cells, the glow-discharge self-sustaining H_2^+ plasma was generated in a direct current mode at energy of 1 keV. A potential difference of 1 to 1.4 kV was created between the anode and an uncoated part of the sample used as the cathode. H_2^+ current density was 1.5 mA/cm^2 with a cathode voltage of –1 kV. The plasma treatments of SCs were performed for 5 and 15 min. The flux density of H_2^+ ions on the SC surface was ~ $8 \cdot 10^{18}$ cm^{-2}.

The phase composition and crystalline structure of the obtained instrument structures was studied by X-ray diffraction. Diffraction patterns were registered on a DRON-4-07 diffractometer in the θ–2θ scanning mode in the radiation of a Cu anode with digital registration. The diffraction patterns were processed using the New_Profile 3.5 software package.

The preferential orientation of the films was studied by analytical processing the diffraction maxima registered using Bragg-Brentano focusing, and the texture coefficient C_i was calculated [12]:

$$C_i = \frac{NI_i}{I_{i0}\sum_{i=1}^{N} I_i / I_{i0}}, \quad (1)$$

where I_i is the integrated intensity of the detected i-peak; I_{0i} is the integrated intensity of the i-th peak, according to the ASTM table; N is the number of diffraction maxima detected in the analysis (reflections corresponding to multiple indices are not taken into account).

To determine the degree of texture of the samples, the parameter G was calculated:

$$G = \sqrt{\sum_{1}^{N} (C_i - 1)^2 / N}. \quad (2)$$

The precision determination of the lattice parameter of the base layers of cadmium telluride was carried out using the Nelson-Riley extrapolation function $f(\theta) = (\cos^2\theta/\sin\theta + \cos^2\theta/\theta)/2$.

The output parameters and the efficiency of the experimental SCs samples were investigated by the light I–V characteristic under illumination conditions AM1.5 at a light flux power of 100 mV/cm^2.

3. Results and discussion

3.1 The structure of the samples in the initial state

Two series of samples were investigated in the work. Samples of the first series (hereinafter referred to as samples No. 1) had a CdTe layer thickness of 3.8–4 μm and further, the samples of this series were irradiated with UV and hydrogen plasma for 5 min. In samples of the second series (herein-

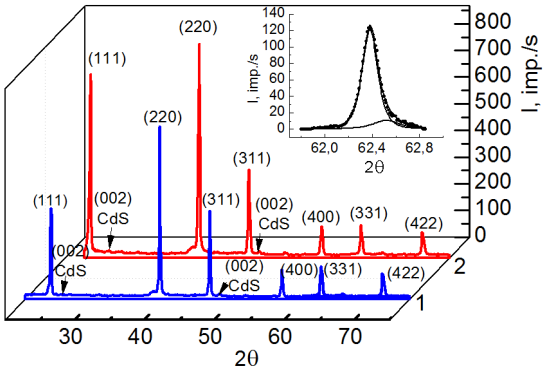

Fig. 1. Diffraction pattern of a sample of solar cells, series No. 1; *1* — in the initial state, *2* — after treatment with hydrogen plasma.

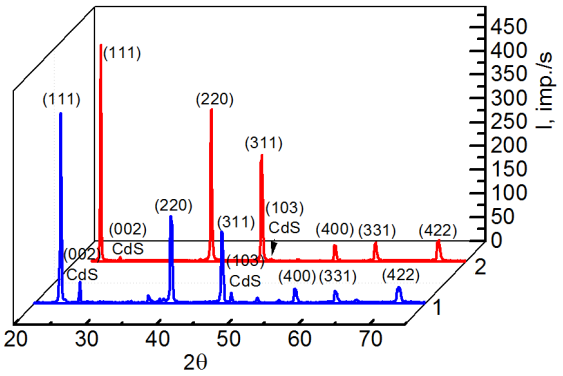

Fig. 2. Diffraction pattern of a sample of solar cells, series No. 2; *1* — in the initial state, *2* — after treatment with hydrogen plasma.

after referred to as samples No. 2), for a more detailed study of changes at the CdS/CdTe interface, the thickness of the CdTe layer was 3 μm due to reducing the duration of the deposition process to 5 min. The duration of annealing during the chloride treatment was also increased to 30 min. The samples of this series were irradiated with hydrogen plasma for 15 min.

Figures 1 and 2 (lines 1) show typical diffraction patterns for samples of these series in the initial state. The diffraction patterns contain reflections from the planes (111), (220), (311), (400), (331) and (422) of stable cubic modification of the cadmium telluride base layer. The diffraction patterns also contain reflections (002), (103) of the hexagonal modification of CdS. It is seen that for samples of both series, all peaks belonging to the CdTe phase are doublets (see, inset in Fig. 1); from the side of large angles, there is a component of lower intensity. The shapes of both components of the reflection are the same, and the value of the integral width differs slightly. This indicates the presence of a secondary phase with the same lattice symmetry, but with a lower lattice parameter. In a number of works (see, for example, [13]) it was experimentally shown that during the formation of CdTe–CdS film heterosystems by vacuum methods, solid solutions are formed due to interfacial interaction.

According to the state diagram of the CdTe–CdS system, at temperatures above 700°C, the maximum solubility of sulfur in

Table 1. Results of processing a typical diffraction pattern for the SC sample of series No. 1 in the initial state/after irradiation with hydrogen plasma

hkl		*d*	Integral intensity, *I*	Integral width, *B*	C_i
[111]	F1	3.7473/3.7436	24.0/52.1	0.141/0.132	0.14/0.30
	F2	3.7411/3.7315	7.8/19.3	0.144/0.131	0.23/0.43
[220]	F1	2.2932/2.2917	76.6/102.0	0.145/0.166	0.76/0.98
	F2	2.2895/2.2841	14.8/11. 9	0.148/0.168	0.73/0.44
[311]	F1	1.9556/1.9549	57. 8/35.6	0.21/0.182	1.15/0.68
	F2	1.9519/1.9488	26.6/19.5	0.212/0.182	2.62/1.44
[400]	F1	1.6210/1.6204	15.1/14.9	0.198/0.209	1.50/1.42
	F2	1.6182/1.6150	1.9/3.5	0.205/0.182	0.91/1.29
[331]	F1	1.4873/1.4871	22.8/22.4	0.195/0.203	1.36/1.29
	F2	1.4852/1.4825	3.0/5.4	0.198/0.209	0.88/1.19
[422]	F1	1.3234/1.3230	18.3/23.2	0.201/0.257	1.09/1.33
	F2	1.3212/1.3188	2.2/5.5	0.196/0.228	0.64/1.22
	F1	G_1 = 0.45/0.40			
	F2	G_2 = 0.76/0.41			

Table 2. Results of processing a typical diffraction pattern for the SC sample of series No. 2 in the initial state/after irradiation with hydrogen plasma

hkl		*d*	Integral intensity, *I*	Integral width, *B*	C_i
[111]	F1	3.7470/3.7483	56.4/50.3	0.171/0.154	0.84/0.65
	F2	3.7326/3.7369	12.1/43.0	0.156/0.124	0.33/0.11
[220]	F1	2.2931/2.2939	32.0/46.4	0.236/0.176	0.80/1.0
	F2	2.2850/2.2872	10.0/12.2	0.211/0.131	0.46/0.53
[311]	F1	1.9560/1.9574	25.3/24.3	0.22/0.150	1.26/1.04
	F2	1.9481/1.9521	12.4/22.2	0.202/0.215	1.14/1.95
[400]	F1	1.6215/1.6233	6.1/6.1	0.302/0.238	1.51/1.31
	F2	1.6153/1.6184	3.3/2.6	0.297/0.244	1.51/1.15
[331]	F1	1.4874/1.4882	4.2/6.8	0.225/0.256	0.63/0.88
	F2	1.4818/1.4841	3.5/3.3	0.291/0.256	0.97/0.88
[422]	F1	1.3235/1.3239	6.4/8.8	0.241/0.259	0.96/1.13
	F2	1.3187/1.3199	57/51	0.296/0.256	1.58/1.35
	F1	$G_1 = 0.30/0.20$			
	F2	$G_2 = 0.48/0.59$			

cadmium telluride layers is 20 % [14]. In this case, CdS_xTe_{1-x} ($x < 0.2$) has a sphalerite structure, and, as the sulfur concentration increases, the lattice parameter of the solid solution decreases according to Vegard's law. The maximum solubility of tellurium in cadmium sulfide layers is 10 %. $CdTe_yS_{1-y}$ ($y < 0.1$) solid solutions have a wurtzite structure. In [15], the presence of the solid solutions was established by the separation of diffraction peaks.

Taking into account the above, we believe that the separation of the diffraction peaks of the studied samples is due to the formation of a layer of CdS_xTe_{1-x} solid solutions, which have smaller interplanar spacings *d* (Table 1).

In the initial state, the lattice parameters of cadmium telluride and solid solutions were 6.481 Å and 6.470 Å, respectively, for the samples of series No. 1 (Fig. 3a lines 1 and 2). In accordance with the Vegard rule, the sulfur concentration in the solid solutions should be 1.7 %. The ratio of the integral intensities of the peaks belonging to CdS_xTe_{1-x} and CdTe is 0.26.

An analysis of the pole density (Table 1) shows that for the main phase (i.e, for CdTe) in the samples of series No. 1, a slight preferential orientation in the [400] direction is observed, while for solid solutions there is a noticeable preferential orientation in the [311] direction. At the same time, a value of G less than 1 for both phases means the absence of texture in the sample.

The lattice parameter for cadmium telluride in the samples of series No. 2 in the initial state was 6.482 Å, which practically coincides with the value for the samples of series No. 1 (the difference is 0.025 %). For CdS_xTe_{1-x} solid solutions, the lattice parameter was 6.458 Å (Fig. 3b lines 1 and 2). In accordance with the Vegard rule, the sulfur concentration in solid solutions for this sample should be 3.7 %, which is significantly higher than for the samples of series No. 1. Such changes are due to a change in the "chloride" treatment regime, as a result of which the formation of solid solutions at the CdS/CdTe interface actually occurs. In addition, for the samples of series No. 2, a decrease in the thickness of the CdTe base layer led to an increase in the intensity of CdS peaks by about 2.6 times, and the ratio of the integral intensity of the peaks of solid solutions and CdTe increased to 0.36.

An analysis of the pole density (Table 2) shows that for the main phase (i.e., for CdTe) there is an insignificant preferential orientation in the [400] direction; and for solid solutions, except for [400] there is an insignificant preferential orientation in the [422] and [311] directions. At the same time, a value of *G* less than 1 for both phases means the absence of texture in the sample.

A comparative analysis of the integral widths of the peaks shows that both phases have approximately the same degree of structural perfection in the samples of both

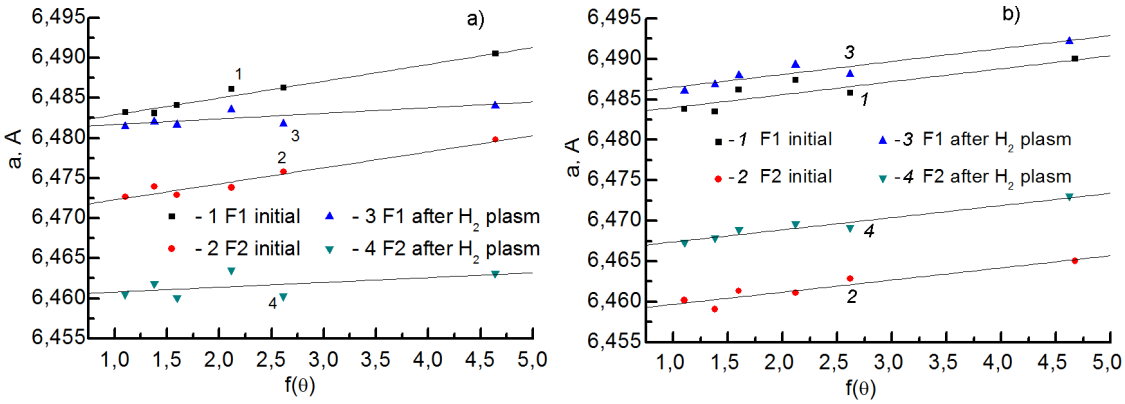

Fig. 3. Precise determination of the lattice parameter in the initial state: a) sample of a series No. 1, b) a sample of a series No. 2; lines 1 and 2 — in initial state, lines 3 and 4 — after irradiation with hydrogen plasma.

series (Tables 1 and 2). Absolute values of the integral width indicate a low degree of defectiveness of the film grains and the best structural perfection of the base layer of the samples of series No. 1 compared to series No. 2, which is associated with a change in the "chloride" treatment mode.

3.2 The structure of the samples after irradiation

In the study of the crystal structure of SCs based on cadmium sulfide and telluride and obtained by the QCV method, no noticeable changes in the crystal structure of the layers were detected after UV irradiation. This is due to a rather high degree of structural perfection of the samples in the initial state, in contrast to CdTe samples made by magnetron sputtering [16] and consisted of a metastable hexagonal modification, which is more sensitive to UV irradiation.

During the irradiation with low-energy hydrogen plasma, etching of the back contact occurred; so that after irradiation for 5 minutes, the central part of the contact, approximately 20 % of its initial area, was etched off, and the rest of the contact became thinned. After irradiation for 15 minutes, the back contact was completely etched.

Figures 1 and 2 (lines 2) show typical diffraction patterns of samples after irradiation with low-energy hydrogen plasma: for samples of series No. 1, the interplanar spacings decreased.

An analysis of the pole density for the sample No. 1 (Table 1) shows that after irradiation with hydrogen plasma, a slight preferential [400] orientation, which was observed for both phases in the initial state, decreased; and for solid solutions, the preferential [311] orientation disappeared. The irradiation leads to a change in the integral width of the peaks of both phases. For the reflection (422) located at the largest diffraction angle, the integral width slightly increases, while at small angles, a decrease in the integral width for the reflection (111) is observed. The intensities of the (111) and (220) reflections increase as well. This indicates a slight increase in the size of coherence lengths and micro-stresses for both phases after irradiation with hydrogen plasma.

After irradiation with hydrogen plasma in the samples of series No. 1, the lattice parameter of the base layer did not change and remained equal to 6.481 Å while the lattice parameter of solid solutions decreased to 6.460 Å (Fig. 3a) lines 3 and 4). In accordance with the Vegard rule, this change indicates an increase in the sulfur content in CdS_xTe_{1-x} to 3.2 %. The reason may be the diffusion of sulfur from the CdS layer when the sample is heated by irradiation.

A decrease in the integrated intensity of the CdS diffraction peaks after irradiation by almost a factor of two in comparison with the initial state also indicates a decrease in the CdS layer thickness due to its dissolution in CdTe. The ratio of the integral intensity of the peaks belonging to CdTe and CdS_xTe_{1-x} before and after irradiation is 0.26, which indicates that the number of solid solutions does not change during irradiation. Also, an increased scatter of points relative to the trend line is observed on the plot for the precise determination of the lattice parameter of the solid solutions after irradiation; this may be due to the formation of packing defects (see Fig. 3a).

For samples of series No. 2 after irradiation, the interplanar spacings in all directions increase, which may be due to the

penetration of hydrogen into the lattice. An analysis of the pole density (Table 2) shows a decrease in the slight preferential orientation [400] for both phases after irradiation with hydrogen plasma, while for solid solutions, a preferential orientation [311] appeared. At the same time, for the main phase, the overall degree of disorientation increased.

A comparative analysis of the integral widths of the peaks of both phases (Table 2) shows that they have approximately the same degree of structural perfection as in the initial state. A comparison of the absolute values of the integral width before and after irradiation with hydrogen plasma indicates a decrease in the degree of defectiveness of grains for any orientation relative to the plane of the film surface (except for the direction [311] for solid solutions). A decrease in the integral width may indicate annealing of defects such as dislocations and twins during the irradiation. At the same time, in the sample No. 2, the lattice parameter increases to 6.485 Å for the base layer and to 6.466 Å for solid solutions, after irradiation with hydrogen plasma (Fig. 3b) lines 3 and 4); while there is no significant change in the peak broadening (Table 2). This change in the lattice parameter for the CdS_xTe_{1-x} phase, in accordance with the Vegard rule, indicates a decrease in the sulfur concentration in solid solutions. However, for samples of this series, a significant decrease in the peak intensity of the CdS phase is observed while maintaining the ratio of the integral intensities of the peaks of the CdTe and CdS_xTe_{1-x} phases (the difference is 3.3 %). That is, as for samples of series No. 1, the dissolution of CdS in CdTe is observed, which should cause a decrease in the lattice parameter.

Two processes affecting the changes in the lattice parameter of solid solutions can be proposed. The first is the dissolution of CdS followed by the formation of solid solutions with higher sulfur contents without a significant increase in the number of them. This process leads to a decrease in the lattice parameter until the maximum solubility is reached. The second is the saturation of the layer of solid solutions with hydrogen, which leads to an increase in the lattice parameter.

For samples of series No. 1, the irradiation time was 3 times shorter compared to samples No. 2, and the contact etching under the influence of plasma was only in the beginning. Therefore, hydrogen was unable to penetrate deep enough to noticeably affect the lattice parameters of the main

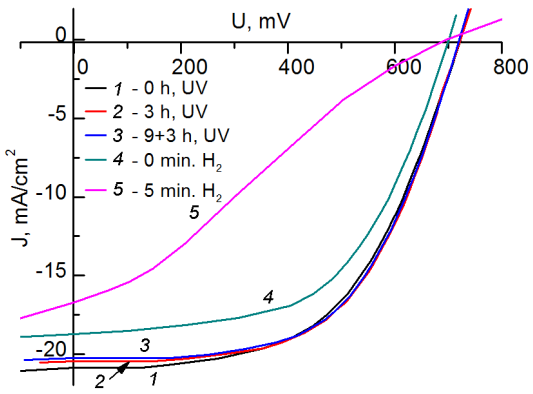

Fig. 4. Typical light I–V characteristics of solar cells before (curve *1*) and after UV irradiation (curves *2* and *3*), before (curve *4*) and after irradiation with hydrogen plasma (curve *5*).

phase and solid solutions; in this case the first process prevailed, namely, the dissolution of CdS due to the concomitant heating of the structure during irradiation. This led to a decrease in the lattice parameter for solid solutions, while for the base layer it remained constant.

For the sample of series No. 2 subjected to a large irradiation dose, the second process prevailed, i.e. hydrogen saturation compensated for the change in the lattice parameter caused by the dissolution of sulfur in CdTe. Obviously, in this case, the application of the Vegard rule is not correct, since the lattice parameter of the main phase increases also due to a high concentration of hydrogen penetrating into the lattice at a high irradiation dose. Solid solutions are located at a depth of about 4 μm from the surface onto which the flux of hydrogen plasma falls.

At the energies used, the mean free path of H_2^+ ions is about 0.1 μm. Despite this, the relative change in the lattice parameter of the solid solutions is significantly larger than the relative change in the parameter of the main phase. Perhaps the reason is the abnormal diffusion of hydrogen, which is observed at high surface doses, as was shown in [17, 18]. Hydrogen accumulates near the CdS/CdTe interface and to a greater extent affects solid solutions localized there. Changes in the entire volume of the layer lead to a change in the lattice parameter without the accumulation of micro-stresses since broadening of reflections is not observed.

3.3 Photovoltaic research results

Figure 4 (lines 1, 2 and 3) and Table 3 show typical light I–V characteristics and

Table 3. Light diode characteristics and output parameters of the glass/FTO/CdS/CdTe/Cu/Au solar cells manufactured in QCV, before and after exposure to low-energy hydrogen plasma and UV irradiation

Output parameters and light diode characteristics	Exposure time of UV irradiation			Exposure time of hydrogen plasma	
	0 h.	3 h.	3 + 9 h.	0 min.	5 min.
J_{sc}, mA/cm^2	21.1	20.6	20.4	18.7	16.8
U_{oc}, mB	722	720	720	700	690
FF, a.u.	0.546	0.573	0.575	0.559	0.287
η, %	8.32	8.48	8.44	7.34	3.06
J_{ph}, mA/cm^2	21.4	20.67	20.5	18.99	
R_s, Oh·cm^2	5.5	4.4	5.0	5.19	
R_{sh}, Oh·cm^2	410	850	740	408	
A, a.u.	2.839	2.992	2.722	2.6878	

output parameters of the solar cells before and after UV irradiation. The light I–V characteristics were measured within a few hours after irradiation; from these the output parameters were determined. As can be seen, the UV irradiation leads to a slight (about 0.16 absolute %) increase in the efficiency of solar cells. Perhaps this behavior is associated with the filling of deep traps with nonequilibrium charge carriers generated upon irradiation of the sample and the formation of unstable point defects under the influence of UV radiation; these defects relax after the exposure is finished. Based on the results of structural and electrical studies, it can be expected that hard UV irradiation will not lead to significant degradation of solar cells based on CdS/CdTe for a long (more than 10 years) period of their operation in outer space.

Figure 4 (line 4 and 5) shows the light I–V characteristics of a solar cell before and after irradiation with hydrogen plasma, and Table 3 contains its output parameters. As can be seen, after irradiation, the working section of the I–V characteristic becomes triangular; therefore, only the output parameters can be determined for SC after irradiation. But an analysis of the type of the I–V characteristics suggests that the diffusion of hydrogen to the separating barrier is not the main critical factor of the observed degradation of the solar cells. This assumption is based on the fact that the open circuit voltage after irradiation decreases slightly. The short circuit current density also drops slightly. The main factor of degradation is the destruction of the back contact, which leads to a significant increase in the series resistance.

4. Conclusions

It was found that the structural characteristics of the base layer of CdS/CdTe based solar cells and their photoelectric characteristics obtained by the QCV method, are practically insensitive to irradiation with UV (at quantum energies 10 eV). It is shown that the effect of exposure to low-energy hydrogen plasma is reduced to two factors. Firstly, it is the heating of the sample and etching of its surface, which occur at high flux densities. Secondly, this is the diffusion of hydrogen, which can be anomalous at high irradiation doses; it is manifested in the formation of the region of maximum hydrogen concentration at a considerable depth from the surface. The result of irradiation also depends on the initial state of the sample, but ultimately, the main effect of irradiation is a change in the composition of solid solutions at the CdS/CdTe interface and an increase in the lattice parameter of the base layer at high irradiation doses.

The studies have shown that SCs based on telluride and cadmium sulfides can withstand radiation effects exceeding in intensity the corresponding effects in outer space (at least in the Earth's orbit). The failure of such solar cells occurs when their physical destruction begins.

References

1. S.Pisoni, M.Stolterfoht, J.Lockinger et al., *Scien. Techn. Adv. Mater.*, **20**, 786 (2019).
2. N.P.Klochko, O.V.Lukianova, V.R.Kopach et al., *Solar Energy*, **134**, 156 (2016).
3. T.Feurer, B.Bissig, T.P.Weiss et al., *Scien. Techn. Adv. Mater.*, **19**, 263 (2018).

4. N.P.Klochko, K.S.Klepikova, I.I.Tyukhov et al., *Solar Energy*, **120**, 330 (2015).
5. N.I.Klyui, V.G.Litovchenko, V.P.Kostylyov et al., *Opto-Electronics Rev.*, **8**, 406 (2000).
6. N.I.Klyui, V.G.Litovchenko, I.P.Lisovsky et al., *Ukr. J. Phys.*, **56**, 461 (2011).
7. N.I.Klyui, Yu.P.Piryatinskii, V.A.Semenovich, *Mater. Lett.*, **35**, 334 (1998).
8. D.L.Batzner, A.Romeo, M.Dobeli et al., in: Proc. 29th IEEE Photovoltaic Specialists Conference; New Orleans, LA; United States; (2002), p.02CH37361.
9. G.Yang, E.W.Cho, Y.J.Hwang et al., *Energy Technology*, **4**, 1463 (2016).
10. M.Kharchenko, *Phys. Chem. Solid State*, **8**, 718 (2007).
11. B.T.Boiko, M.Kharchenko, in: Proc. XII International Conference on Physics and Technology of Thin Films and Nanosystems (ICPTTFN-XII), Ivano-Frankivsk, Ukraine (2009), p.277.
12. H.R.Moutinho, F.S.Hasoon, F.Abulfotuh, K.Kazmerski, *J.Vacuum Sci. Techn. A*, **13**, 2877 (1995)
13. B.T.Boiko, G.S.Khripunov, V.B.Yurchenko, H.E.Ruda, *Solar Energy Mater, Solar Cells*, **45**, 303 (1997).
14. S.Y.Nunoue, T.Hemmi, E.Kata, *J. Electrochem. Soc.*, **137**, 1248 (1990).
15. B.E.McCandidiess, R.W.Birkmire, in: Proc. 26th IEEE Photovoltaic Special Conference: Proceeding of the International Conference, Anaheim (USA) (1997), p.307.
16. G.I.Kopach, A.I.Dobrozhan, G.S.Khrypunov et al., *Phys. Chem. Solid State*, **20**, 165 (2019).
17. G.D.Tolstolutskaya, A.V.Nikitin, V.V.Ruzhytskyi et al., *PAST*, **102**, 25 (2016).
18. A.V.Nikitin, G.D.Tolstolutskaya, V.V.Ruzhytskyi et al., *J. Nuclear Mater.*, **478**, 26 (2016).